ARUP

CLIC

Geothermal use of tunnels

Technical Report

Reference: ARUP_202204_CERN

| 05 May 2022

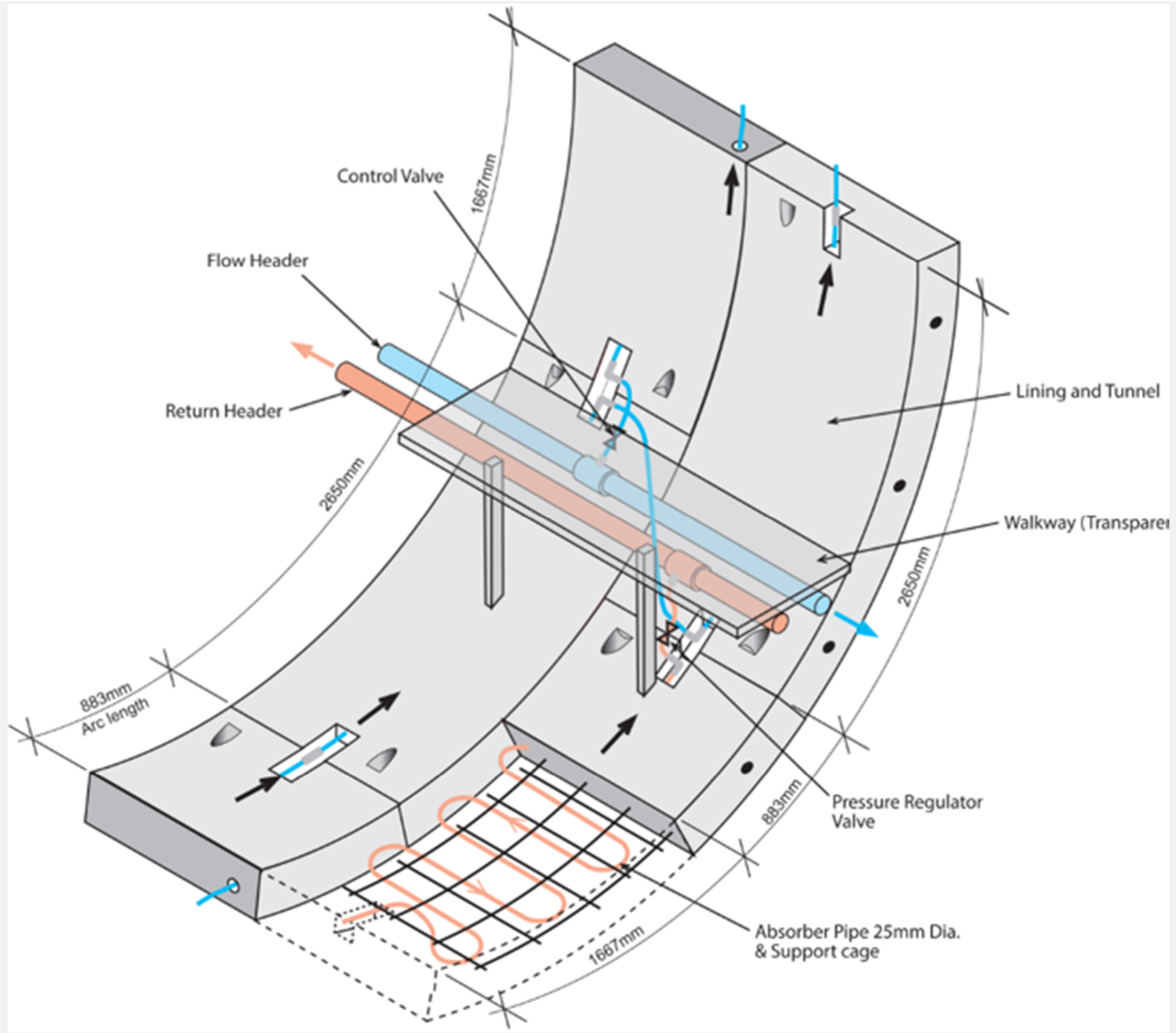

Job number

Ove Arup & Partners Limited
8 Fitzroy Street
London
W1T 4BJ
United Kingdom
arup.com

ARUP

Document Verification

Project title	Geothermal use of tunnels
Document title	Technical report
Job number	252183
Document ref	ARUP_202204_CERN
File reference	

Revision	**Date**	**Filename**			
		Description	Technical feasibility on thermal tunnel, issued on 18/05/2022		
			Prepared by	**Checked by**	**Approved by**
		Name	Alex Q Chen	Duncan Nicholson	Duncan Nicholson
		Signature	[signature]	D.P. Nicholson	D.P. Nicholson
		Filename			
		Description			
			Prepared by	**Checked by**	**Approved by**
		Name			
		Signature			
		Filename			
		Description			
			Prepared by	**Checked by**	**Approved by**
		Name			
		Signature			

Issue Document Verification with Document ✓

Contents

Tables

Figures

Drawings

Pictures

Photographs

Attachments

Appendices

1. Introduction

1.1 Concept of thermal tunnels

From energy source perspective, there are two types of thermal tunnels to consider: one is an open system (hydrothermal), which drainage water (water temperature 7 - 24°C based on existing projections) is used as the energy source. This is typical for tunnels located with a thick rock overburden and groundwater appears in large quantity as tunnel seepage (Stemmle, et al., 2022); the other type is a closed geothermal system which absorber pipes are integrated in the tunnel structure as shown in Figure 1, low enthalpy energy is transfer to or from the ground by circulating heat exchange fluid through the pipes (Nicholson, et al., 2013). This report is on the closed geothermal system of absorber tunnel lining, hereafter referred to as “thermal tunnel”.

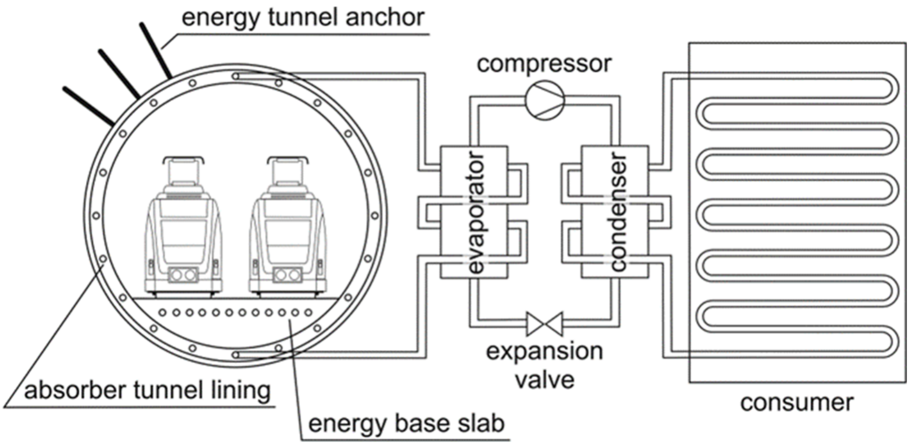

Figure 1 Concept of thermal tunnel (Stemmle, et al., 2022)

The thermal tunnel system harvests heat from the medium that the tunnel lining is interfacing with: both the air or water inside the tunnel, and the soil mass surrounding the tunnel. For clarity, we further divide the tunnels into 2 categories: “cold tunnel” and “warm tunnel”. The concept is shown in Figure 2. The “cold tunnel” has no energy source within the tunnel, air temperature inside the tunnel is similar to the ground ambient temperature or the surface atmospheric temperature if ventilation is good. Short road or rail tunnel would fall into this class. The “warm tunnel” has heat emitting sources inside the tunnel, air temperature inside the tunnel is higher than the ambient ground temperature. For example, metro tunnels or high voltage cable tunnels are belonged to the warm tunnel. The warm tunnels may require ventilation for cooling to keep the tunnel temperature within operational range (Nicholson, et al., 2014).

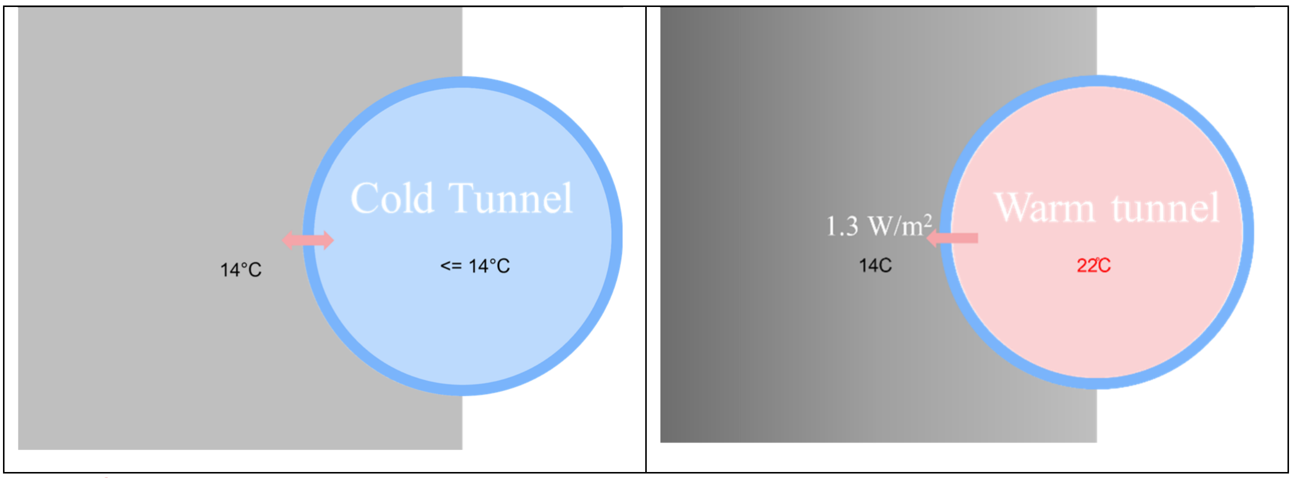

Figure 2 Cold and warm tunnels under natural condition

With no active heat extraction or rejection, there is a natural thermal flux across the tunnel wall in the warm tunnels due to temperature difference. For example, the heat flux per meter of the tunnel through the tunnel wall q (kW/m) can be calculated using the formula below (Bowden, 2003):

$$q = \frac{2\,\pi\,k\,U_0}{\cosh^{-1}(d/r)}$$

Where

d = tunnel depth (m) (120m)

r = tunnel radius (m) (5.6m diameter)

k = combined thermal conductivity of soil and tunnel liner (W/m-K) (2.1W/m-K)

U_0 = tunnel temperature above the ambient soil (K) (22 - 14 = 8°C)

$\cosh^{-1}(x)$= inverse of hyperbolic function cosh(x)

Based on the CLIC settings (listed in the brackets above), q is calculated as 23.7 W/m of tunnel. This equates to 1.35 W/m^2 tunnel surface area. For comparison, geothermal heat flow in southern Switzerland is 0.04 to 0.1 W/m^2.

To take advantage of the large contact area between tunnel and the rock mass, tunnel structure can be thermally activated by imbedding absorber pipes (ground heat exchanger) within the tunnel lining, as shown in Figure 3. This is the basic concept of thermal tunnel (also called energy tunnel, or geothermal tunnel). As expected, when harvesting ground heat by the system, the heat exchange rate will be smaller for the cool tunnel than the warm tunnel. This will be discussed in Section 2.

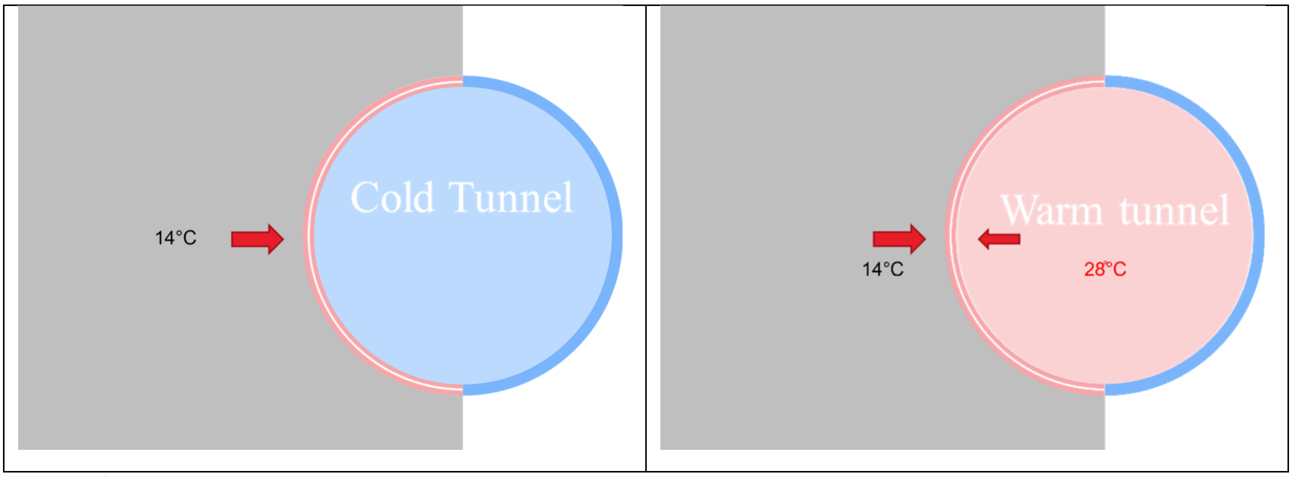

Figure 3 Cold and warm tunnels with absorber pipes embedded in the tunnel liner

Groundwater flow is known to enhance heat exchange efficiency significantly (Barla, et al., 2019). However, groundwater flow is deemed insignificant at CLIC due to the low permeability of the Tertiary Molasse formation, thus it is not considered in this report.

1.2 Crossrail thermal tunnel design

Tunnel adaptation as ground energy structure has been explored since early 2000s (Brandl, 2006; Adam & Markiewicz, 2009; Franzius & Pralle, 2011). Comparing with other forms of closed geothermal systems (boreholes, piles, walls), tunnels have a bigger soil-structure surface and involve a larger volume of ground, the heat exchange rate is expected to be higher.

Arup undertook the tunnel energy lining (TES) design for London's Crossrail tunnels between 2010 and 2012. Crossrail tunnels are of twin tunnel structure of 21km each running across central London in east-west direction. The tunnel is constructed using tunnel boring machine (TBM) with pre-cast tunnel segmental liner, the tunnel depth is 10 to 30m, and the tunnel is most running within the London Clay.

Arup's design is to use strong crossline polyethylene pipes (PEX) manufactured by Rehau Ltd as the heat absorber for better endurance and faster connection. The absorber pipes in each prefabricated segment of a tunnel ring form a ring circuit, this is done by connecting to the pipes of adjacent segments via box out. There are 77 meters of pipes within a ring. Five ring circuits (ring width is 1.6m each) are cross-connected via ring-to-ring connections which are connected to the flow and return headers to form one full loop circuit. A number (50 to 60 nr) of loop circuits can be connected to the same supply and return headers to form a tunnel circuit.

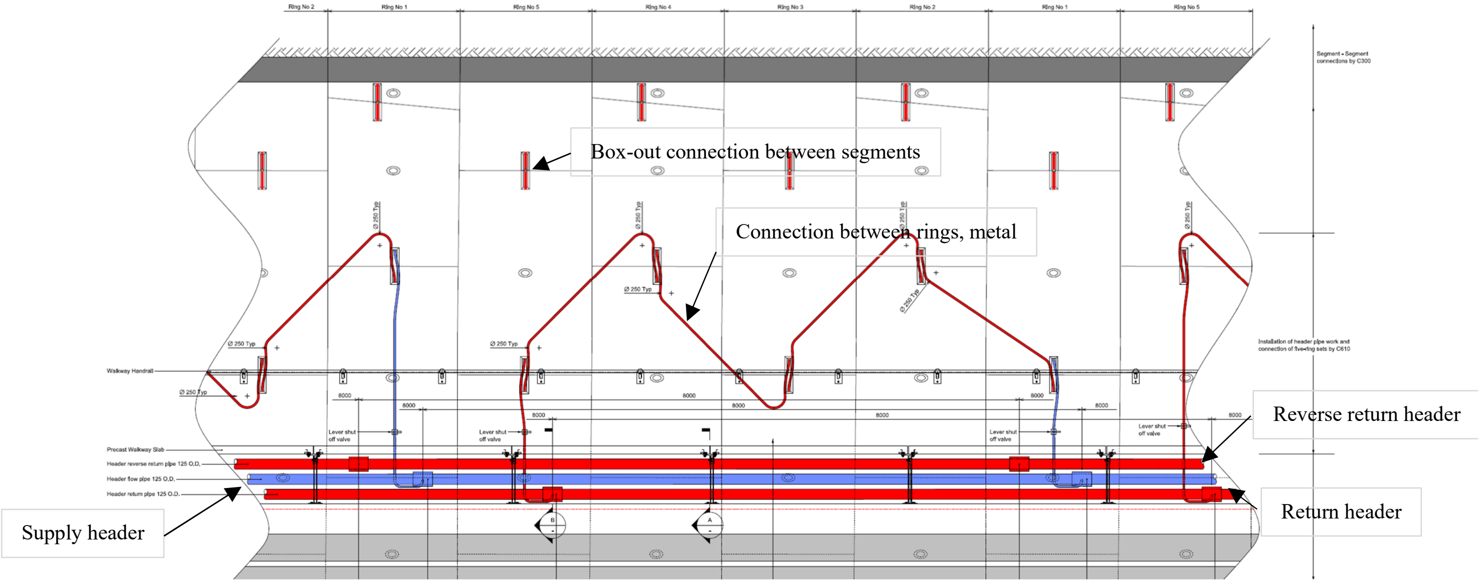

Figure 4 General arrangement of absorber pipes showing a full loop circuit

Arup's design covers from segment production to tunnel lining erection, hydraulic system, fire safety, liner's structural performance, heat distribution to users, and cost benefit analysis etc. Production trial was carried out and fire test was performed. Bespoke designs were developed for two sites (860m tunnel at Fisher Street Shaft, and 800m tunnel at Stephen Green Shaft) (Arup, 2012) to carry out trails of limited tunnel length. However, these trial sections did not go ahead due to contractor's priority and time limitation.

The thermal lining segments exchanges heat from the geological formations by conduction as well as receiving heat flux from the tunnel air. Based on numerical simulations, an extraction rate of 10 to 30 W/m² of tunnel surface can be sustainable with no detrimental thermal impact on liner structure. The design details and considerations are provided in a publication by (Nicholson, et al., 2014) (see appendix A). A 3D finite element model was developed in LS-Dyna which the thermal-mechanical behaviour of the segmental lining was modelled in detail.

1.3 CLIC tunnel

The CLIC site is in the south end of the Swiss Geneva Basin. See Figure 5 for its proposed location. The geology from ground surface down is Quaternary Moraine deposits, Oligo-Miocene Molasse formation, and Cretaceous Limestone formation. Below it lies the Cretaceous, Jurassic, and Triassic formations. Exploration borehole GEO-01 is within the CLIC site boundary. Detail of the geological sequence and cross-sections are presented in Figure 6. Section Y-Y' cuts cross the CLIC.

As shown in Figure 7, the CLIC tunnel is mostly within the Oligo-Miocene Molasse formation at depth between 100-150m. The tunnel intersects the Cretaceous Limestone at its south end where the Jura Mountain rises and Molasse formation thins out.

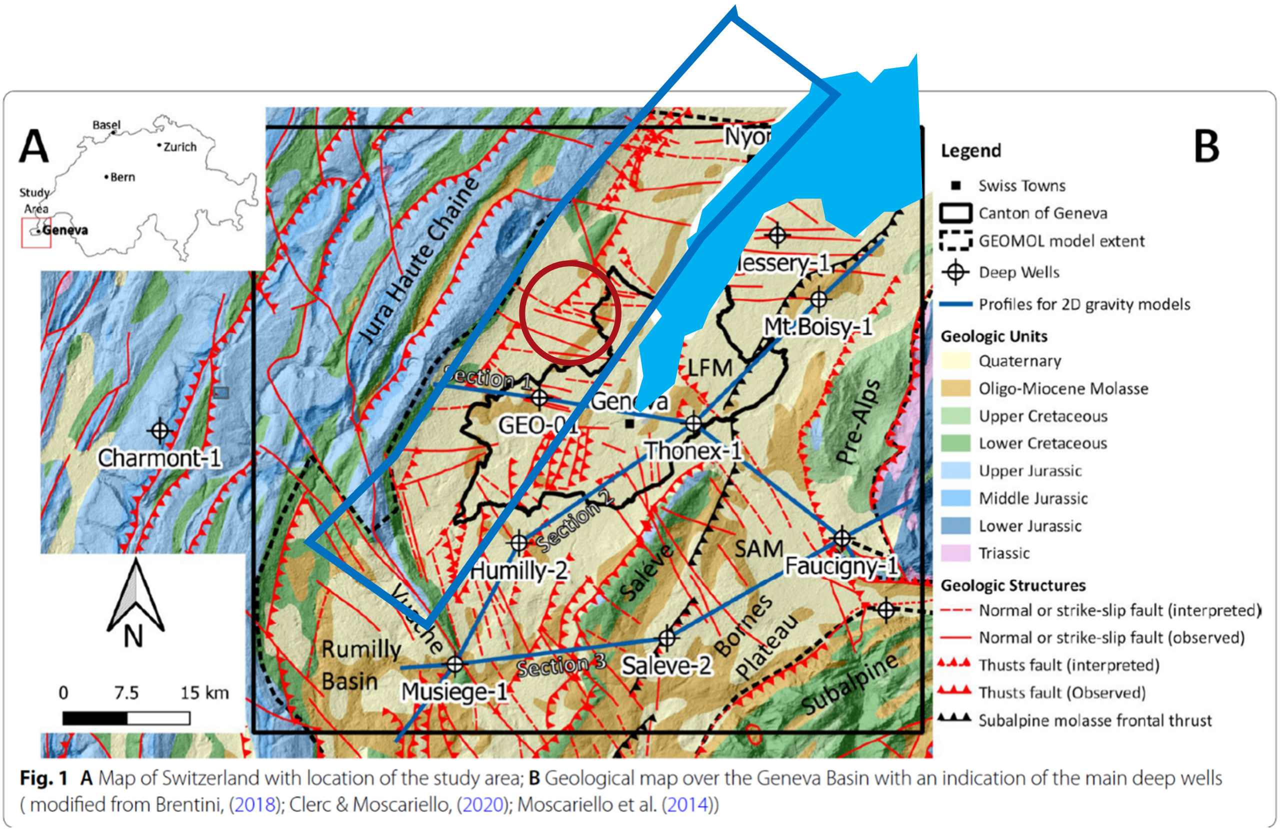

Fig. 1 A Map of Switzerland with location of the study area; B Geological map over the Geneva Basin with an indication of the main deep wells (modified from Brentini, (2018); Clerc & Moscariello, (2020); Moscariello et al. (2014))

Figure 5 Outline of the CLIC zone and the existing LHC superimposed on geology map (from (Guglielmetti & Moscariello, 2021)

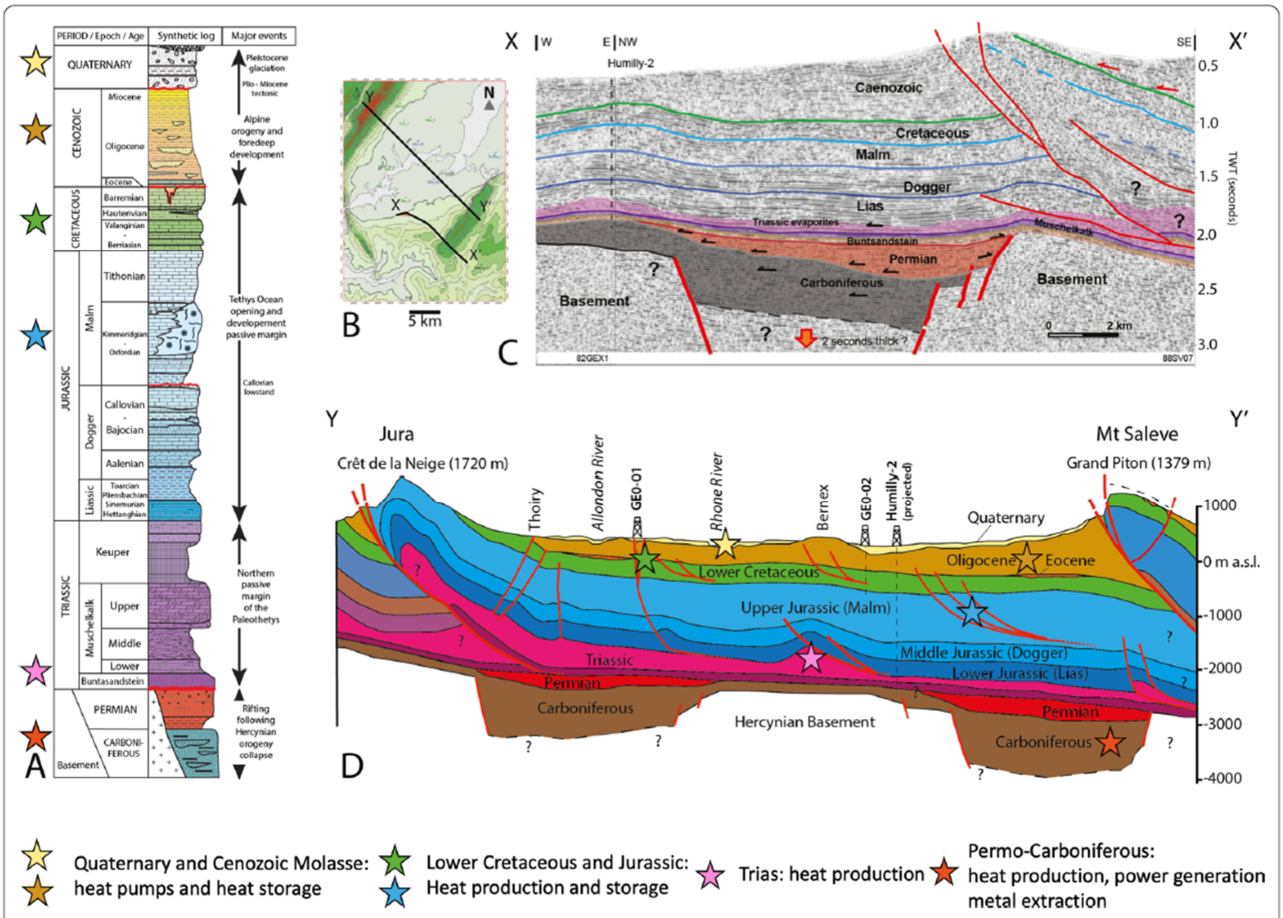

Fig. 2 **A** stratigraphic log of the Geneva Basin and indication of the main geothermal targets; **B** Map across the Geneva Basin showing the traces of the seismic line in panel **C** and of the geologic cross-section in **D**; **C** Seismic profile over the SW sector of the Geneva Basin ((modified from Moscariello, (2019)); **D** Cross-section cutting through the GB (modified from Moscariello, (2019) indicating the main geothermal targets)

Figure 6 Geological cross-section of the Geneva Basin (Guglielmetti & Moscariello, 2021)

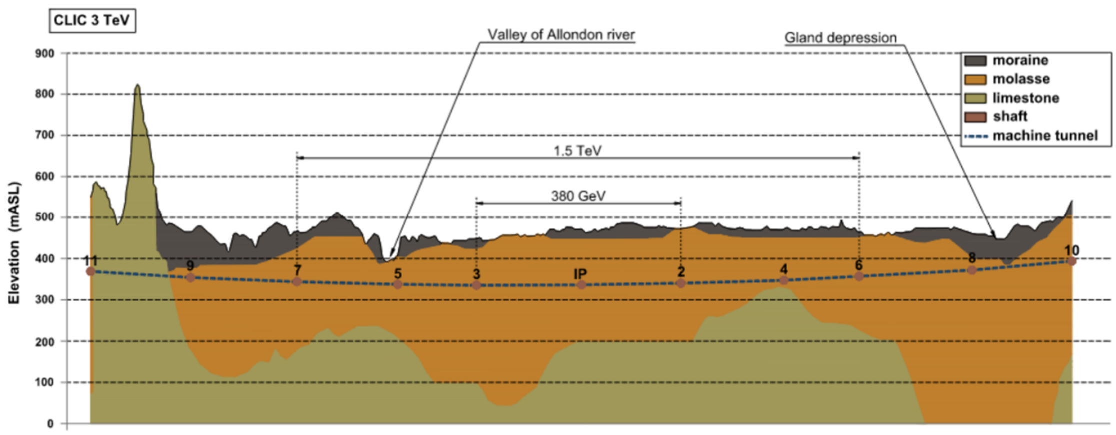

Figure 7 Geology cross-section along the tunnel alignment (CERN, 2018)

The geothermal gradient is between 25 and 40°C/km the Swiss Molasse Basin, described with the highest values in the north, and decreasing to the south (Rybach, 1992). However, reading the geothermal map, the geothermal gradient at the CLIC appears to be > 35°C/km. Borehole GEO-01 (at Long 6.04692, Lat 46.22162) was drilled to 744 m depth into the Upper Jurassic, artesian flow of 55 Litre/s from the Cretaceous and Jurassic formations was of 34°C with 8 bar water head (Guglielmetti & Moscariello, 2021). Assuming ground temperature is 10°C at 10m below ground level, the calculated geothermal gradient at Geo-01 is 36 to 38°C/km, in agreement with the geothermal gradient assumption above.

The average tunnel axis level is on average 120m from surface (Figure 8). Assuming ambient ground temperature of 10°C at 10m depth, and geothermal gradient of 35°C/km, the rock temperature at CLIC tunnel is about 14°C.

The Molasse sediments in Geneva Basin are of low permeability, there are no major aquifers. Groundwater movement is assumed to be insignificant.

There is heat emission at CLIC tunnel from equipment both above and below ground which need to be disposed of (CERN, 2018). CERN has been actively looking for opportunities to reduce carbon footprints for its existing and future tunnels. One way to do so is to recovery the waste heat from warm ventilation air or water. One recent example is the heat recovery project at CERN-P8 where 2no 5MW heat exchangers were installed alongside of cooling towers to warm water to 30°C in a local "anergie" loop and deliver it to the community ZAC 'Ferney-Voltaire' at 2km distance via 400mm diameter pipes with minimum heat loss (Claudet, 2022).

1.4 CLIC tunnel vs Crossrail tunnel

Table 1 lists the conditions at CLIC and Crossrail tunnels. Both tunnels are similar in size, ground temperature, and groundwater condition. The main tunnel at CLIC is of pre-cast segment. Molasse formation has a higher thermal conductivity than the London Clay.

Table 1 CLIC tunnel vs Crossrail tunnel

Parameters	CLIC Main Tunnel	Crossrail Tunnel	References	Comments
Tunnel internal diameter (m)	5.6m typical for the main tunnel	6.2m	CLIC tunnel cross-section drawing CLIC.CE-1.1710.0004	CLIC tunnel diameter is slightly smaller
Tunnel lining type	Precast segmental lining	Precast segmental lining		
Segmental liner design	TBD	7 segments + 1 key stone	(Nicholson, et al., 2014)	TBD – to be decided
Segment thickness (m)	0.3 to 0.4	0.3		
Segment concrete	TBD	C50/60 concrete with steel fibre reinforced		Thermal properties depend on concrete mix
Tunnel depth (m)	54 to 460m, 124m (on average) see Figure 8	15 to 25m	Machine tunnel.csv	Significant hydraulic pressure would be at CLIC tunnel
Main tunnel length (km)	47.7, vent shaft at 5km apart	21 x 2 = 42, vent shaft	(Nicholson, et al., 2014)	
Service tunnel liner	SCL	NA		Detail unknown
Geology at tunnel level	Mostly within the Molasse deposits, Swiss Molasse Basin	London Clay, London Basin		
Lithology	Varies, conglomerates, mudstone, sandstone, marl	Overconsolidated clay or silty clay	Ref-1	Assumed the Molasse Fm is saturated, low permeability

Parameters	CLIC Main Tunnel	Crossrail Tunnel	References	Comments
Geothermal Gradient (°C/km)	35 to 40 (35)	25	Ref-5, Fig 1,	No major aquifer at or above tunnel depth
Ground temperature at tunnel (°C)	14 to 15	14.8 (measured)		Calculated by assuming CLIC ground temp is 10C at 10m depth
Ground thermal conductivity (W/m-K)	2.4	1.8	Ref-5, 7, 9	Lack of site-specific data
Ground thermal capacity (J/kg-K)	900 to 1200	1000	Ref-7, 9	
Concrete thermal capacity (J/kg-K)	700	700	Ref-7	Volumetric heat capacity Svc = 2300 kJ/m^3-K
Tunnel air temperature (°C)	Relatively constant 14 to 22	Variable, 14 to 30	(CERN, 2018)	
Natural geothermal heat flux (W/m^2)	0.04 to 0.1	0.06		
Hydraulic gradient	Very low	Very low		Assumed, ignored in the assessment
Hydraulic conductivity (m/s)	Low	Very low		Assumed, ignored in the assessment
Energy sources	Surrounding rocks, for heating and cooling	Surrounding rocks and tunnel air, for heating only		
Ground heat exchanger loop size	TBD	20mm ID, 25mm OD		assumed

The key differences of the two tunnels are:

- CLIC tunnel is much deeper than the Crossrail tunnel, this will have implications on pipe hydraulics and tunnel lining design,
- Air inside the Crossrail tunnel is frequently heated up by train operations, ground mass behind the tunnel wall is to be warmed up with time; At the CLIC tunnel, the equipment heat is excluded from current consideration. Only the rock mass behind the tunnel wall is considered for thermal storage and thermal movement,
- The Crossrail tunnel is to operate in heating mode only (i.e., heat is extracted from the ground); Whilst the CLIC tunnel can be used for both heating and cooling (though cooling demand is uncertain).

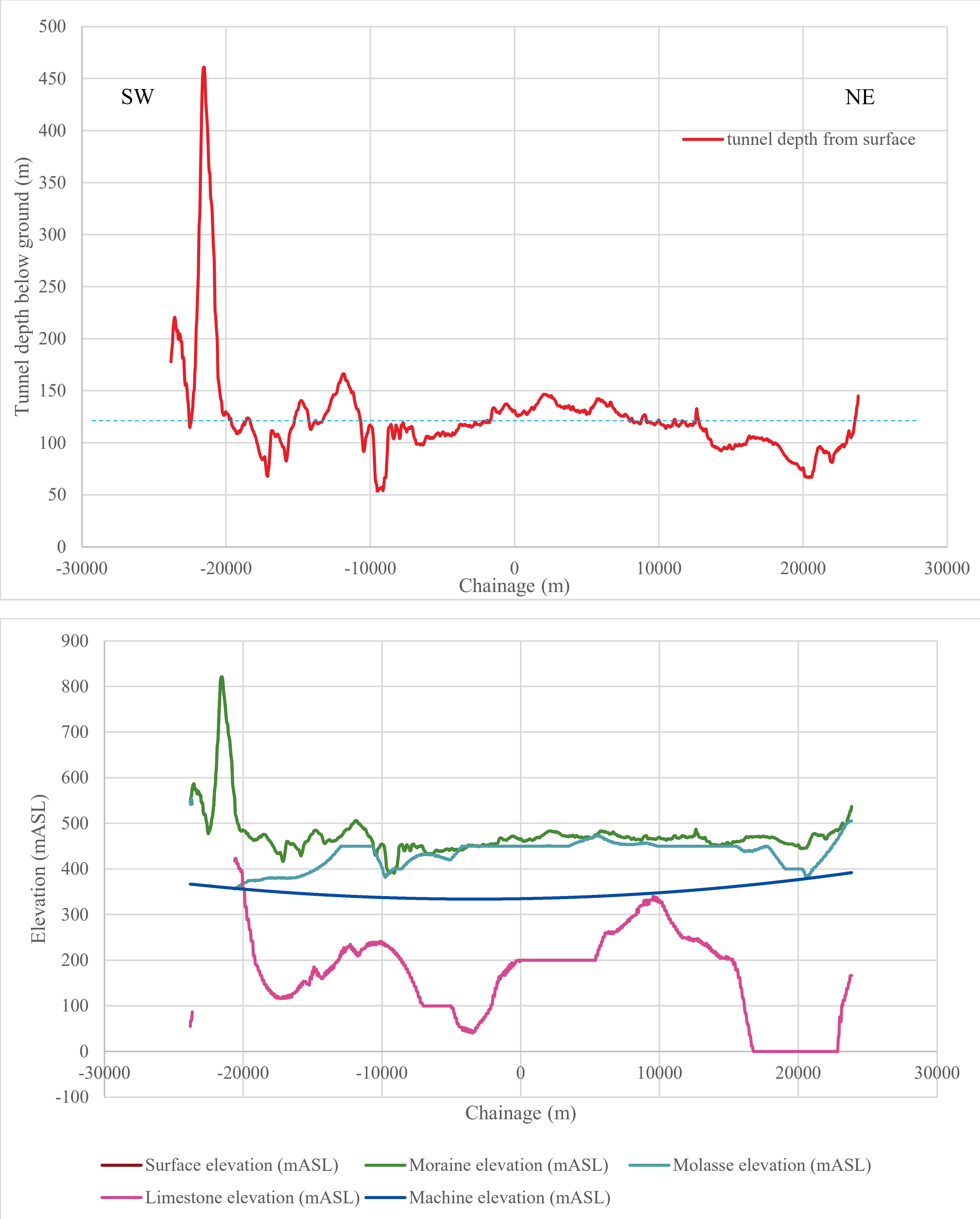

Figure 8 CLIC Tunnel detail

2. Estimate Heat Extraction Rate

A closed ground energy system generally requires a constant ground temperature over the years, the ground operates as a heat source during winter supplying warmth to buildings, and functions as a heat sink during summer when cooling is required. This would result in seasonal fluctuations of ground temperature, however a good system ground temperature shall remain relatively unchanged from one to the next.

2.1 Heat extraction only during winter

The long-term sustainability of ground source energy systems is defined by the net difference in annual heating and cooling. The ground has a finite capacity to extract and absorb heat and when the net imbalance between heating and cooling exceeds this capacity, the efficiency of the system starts to diminish.

An axisymmetric finite difference model was used by (Franzius & Pralle, 2011) to assess thermal response of the soil and carrier fluid. Three operational scenarios were simulated. A fixed temperature boundary is set at 30 m radial distance from the tunnel. The relevant heat transfer equation can be solved using methods such as forward time centre space (FTCS), the backward time centre space (BTCS) or Crank-Nicolson methods. The results are plotted in Figure 9

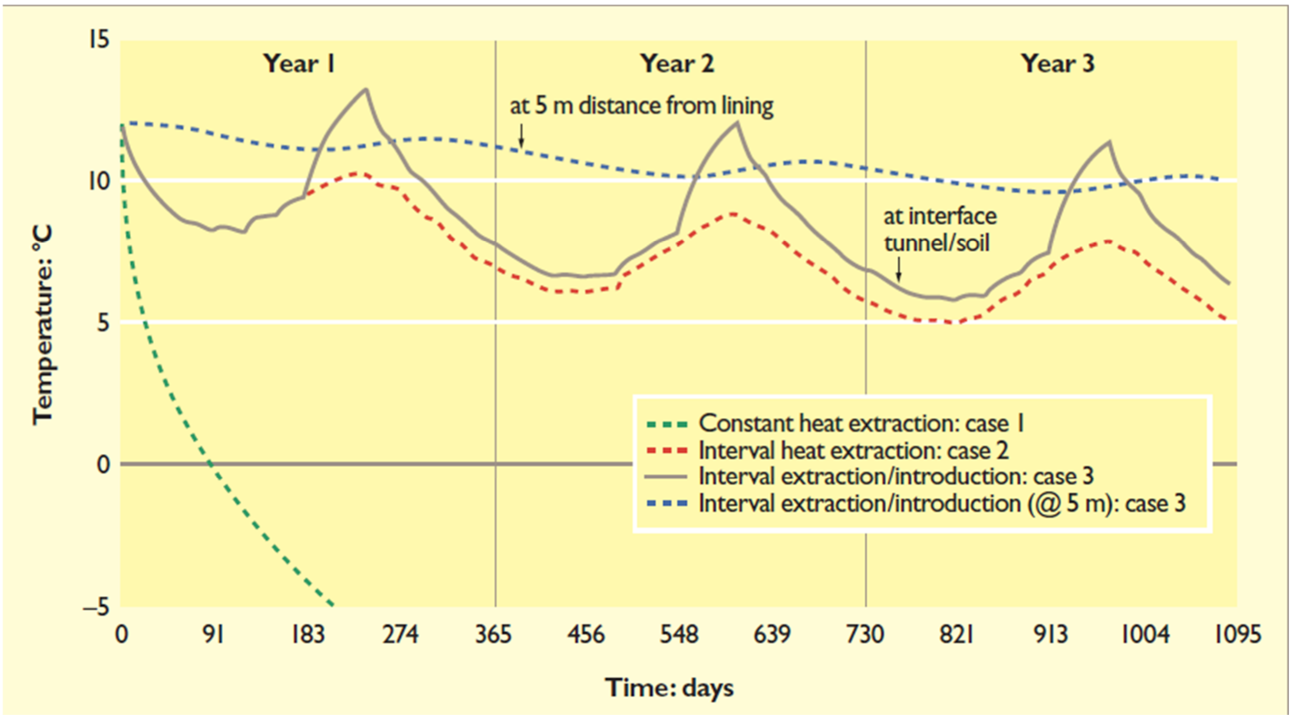

Figure 9 Numerical simulations of a cold tunnel under three cases. Case 1 – continuous heat extraction throughout the year, 24 hours a day; Case 2 – heat extraction for a number of hours per day, and no operation during July and August; Case 3 – heat extraction runs a number of hours per day, and heat rejection during July and August. All heat flux is set to 10W/m^2, the results presented is soil tempeature at tunnel-soil interface.

With little thermal recharge and continuous heat extraction, for case 1 the ground temperature decreases rapidly from 12°C to 0°C within three months. This indicates that the thermal storage of the soil has depleted; The operation is therefore not sustainable. Case 2 is that the heat extraction rate varies with time, from 7.2hrs in January to 1.6hrs in June, and no heating demand in July and August. With 1500 operational hours, heat recharge flux from the fixed temperature boundary may exceed the heat extraction during low operation months, resulting in raising soil temperature from May which peaks by the end of August. Over the annual cycle the total heat extracted is 15 kWh, which exceeds the geothermal recharge in the year, the soil temperature drops, albeit at a slower pace than Case 1, temperature at the tunnel decreases from 12°C in year 1 to 5°C in year 3.

For Case 3, heat rejection was allowed in July and August, the system has a better balance than Case 2, the net heat extraction is the smallest due to heat rejection which represents building cooling. Soil temperature decreases at a slowest pace, temperature at the tunnel drops from 12°C in year 1 to 7°C in year 3, at 5m distance from the tunnel, the temperature is 10°C at the end of year 3.

The above simulations implies that for a cold tunnel 10W/m^2 heat extraction rate with limited operation hours (no more than 900 hrs) may be able to operate over many years without heat rejection. With cooling to balance, the heat extraction operational hours can be prolonged.

2.2 Heat extract in winter and heat rejection in summer

A closed system is sustainable and performs better when the imbalance of heat extraction and injection over a year is minimised. This principle is true for thermal tunnels. Considering the Case 3 above, if the heating rejection is greater and the thermal balance on the ground side is reached, the system is viable.

Given the tunnel air temperature profile in the Geneva basin, it is expected that cooling demand for residential buildings are very small. However, cooling demand for commercial or office buildings may be significant.

If there is no cooling demand, the system can balance the loads by operating in cooling mode during summer and dumping the coolth in the environment.

2.3 Heat extract with warmed tunnel air

CLIC set out design temperature for the following (CERN, 2018):

- Main-Linac tunnel, BDS, detector hall, caverns, dumps and turnarounds: 28°C
- Injectors, Booster, Damping rings, Transfer lines: 22°C

As per the design requirement, the main tunnel temperature is to be 28°C. Our consideration so far has ignored tunnel air input. Higher air temperature will result in heat flux into the wall under nature condition, at a rate around 2.3W/m^2 (See 1.3 for formular)

During operation, the CLIC tunnel would be similar to a “warm tunnel”, equipment heat could result in tunnel temperature rise. Although 90% heat is likely to be removed by tunnel ventilation chilled water system, the air temperature rise in the tunnel will improve the thermal imbalance of the rock mass. It is difficult to quantify the benefits without knowing the operational detail.

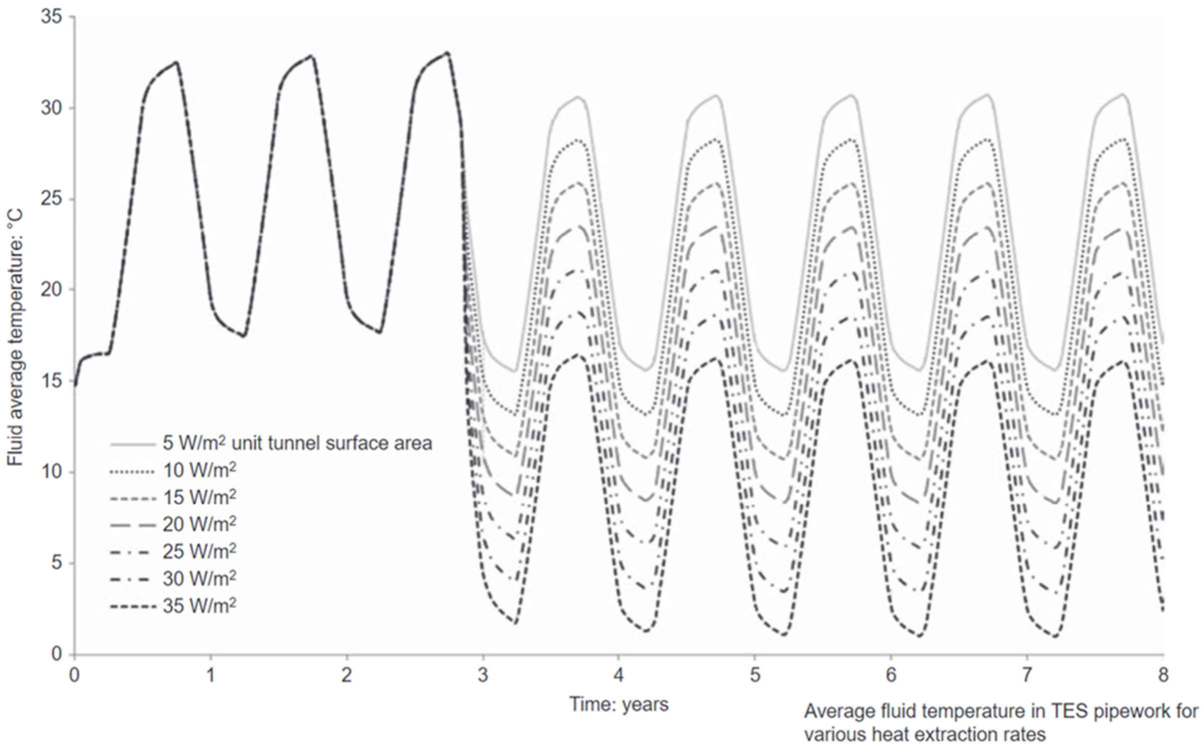

Figure 10 The average circulation fluid temperature at various heat extraction rates when operating continuously. No operation in the first three years (Nicholson, et al., 2014).

Extracting heat has the benefit of cooling the tunnels in case of considerable amount of heat build-up. This not only helps to alleviate tunnel cooling need, but also beneficial to the thermal tunnel system as it helps to balance the thermal mass. A LS-DNYA was constructed for Crossrail where the thermal activation of the segmental lining is modelled in detail. Figure 10 shows that the extracting 20 to 30 W/m^2 continuously is achievable without risking of freezing.

A design chart has been developed for thermal tunnel exchange rate during heat extraction and rejection operation (Barla & Di Donna, 2018). Based on the chart (See Figure 11), the heat exchange rate is around 10 W/m^2 for heating and 20 W/m^2 for cooling under no groundwater flow condition. Note that this chart shall be used with caution, as it focuses on shallow tunnels (21.5m deep in the example) with significant groundwater flow around the tunnel.

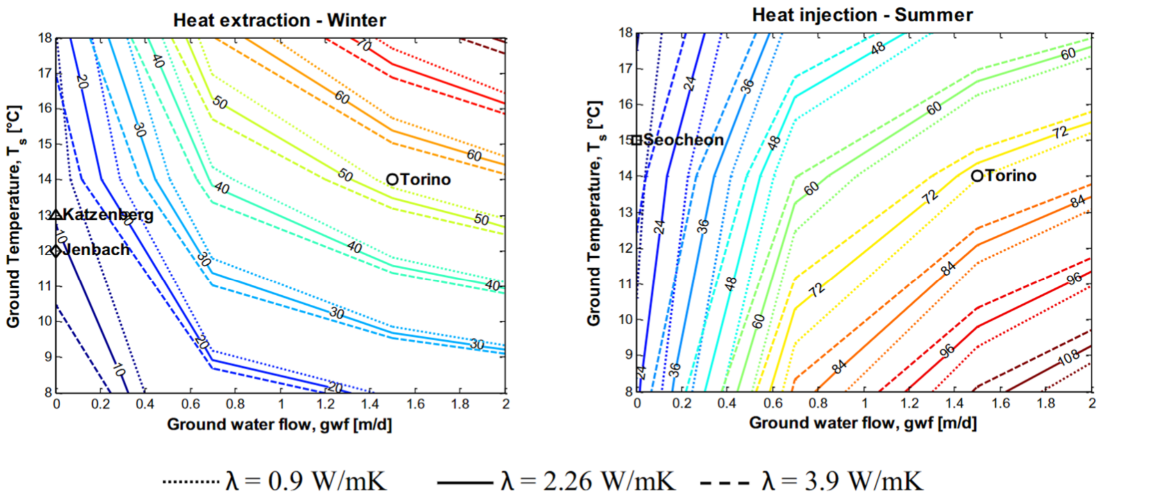

Fig. 5. Design charts for winter mode and summer mode (extracted and injected heat in W/m^2) – (experimental data from Franzius and Pralle (2011) and Lee et al. (2012)). (Di Donna and Barla, 2016).

Figure 11 A design chart to estimate heat extraction and rejection rate for thermal tunnel (Barla & Di Donna, 2018)

2.4 Comparison with closed loop borehole

Based on the heat exchange rate of 10W/m^2, and 600m thermally activated tunnel length, the power output from the tunnel is 105kW. With 3.0 heating COP of heat pump, this system will deliver 158kW to the buildings. For reference, heating demand of a residential housing is 20-40kW.

For a closed loop borehole of 100m deep, the typical heat exchange rate is 30W/m, a geothermal borehole will yield 3kW. To run the closed loop borehole sustainability, both heating and cooling demands are requirement.

Therefore, a 600m tunnel will be equivalent to 35nr. closed loop geothermal boreholes, or better 3500m borehole length as the depth of closed loop boreholes could vary between 100 to 200m. This comparison has not taken the benefit of thermal balance of the tunnel. While it is a necessary for closed loop borehole to be operated with balanced loads. If the tunnel is run with balanced load as the ground source boreholes do, the output can be 20 to 30 W/m^2 (use 20 W/m^2), a 600m tunnel would be equate to 70nr 100m boreholes.

Table 2 lists the estimate of energy outputs for scenarios with heat rejected and heat flux from tunnel air.

Table 2 Estimated thermal tunnel energy outputs

Parameters	Heat extraction for 1200hr per year	Heat extraction for 1200hr/yr and heat rejection for 600hr/yr. Cold Tunnel	Heat extraction 1200hr/yr and rejection 900hr/yr. Warmed tunnel air occasionally	Heat extraction for 1200hr/yr. And heat rejection 900hr/yr, continuously warmed air	Comments
Heat extraction rate (W/m^2	10	15	20	30	based on LS-DYNA and FTSC simulations

tunnel surface)					
Tunnel internal diameter (m)	5.6	5.6	5.6	5.6	CERN
Thermally activated tunnel length (m)	600	600	600	600	limited by hydraulic loss, pipe pressure and space proofing inside tunnel and shaft
Total tunnel area (m^2)	10,556				
Heat output at (kW)	106	158	211	317	
COP for heating	3.0				COP 3 for heating
Heat delivered to buildings (kW)	158	238	317	475	Including heat pump inputs

For using the tunnel heat to space heating, a small house in the UK needs $5kW^{th}$, based on $10W/m^2$, therefore a 600m tunnel is able to provide heat to 30 to 60 nr flats. For a residential building, heat demand is 20 to $40kW_{th}$, a same length tunnel is able to provide heat for a few buildings .

3. Thermal Tunnel Design Considerations

3.1 Segmental tunnel

3.1.1 Hydraulic pressure and head loss

A PE100 pipe has a pressure rating of 16 bar. To connect the tunnel system with surface, a hydraulic break is needed. This may be achieved by using plate heat exchangers at the tunnel which connect the flow and return pipes from the surface (secondary circuitry) on one side and the tunnel thermal circuitry on the other side. Depending on the pipe arrangement, one tunnel circuitry can be 300 to 600m in tunnel length. A surface access structure (e.g., vent shaft) can connect one or two tunnel circuitries.

The pipe in the segment is formed with tight bending radii to maximise the absorber pipe length. In the Crossrail case, the bending radii is 150mm. For CLIC each ring may contain up to 70m long pipes. The total length of absorber pipes per 100m tunnel is to be up to 4,300m.

Flow rate is a key factor in determining hydraulic loss and thermal exchange rate, pipe joints, fittings and bends all result in hydraulic loss. To minimise hydraulic loss, the flow rate shall be maintain at a low but in a turbulence state for higher heat exchange efficiency.

3.1.2 Fire Safety in CLIC

Flammable material, such as plastic pipes, may be banned from CLIC tunnel. When the pipes are embedded in the concrete mass, its fire hazard is reduced and is generally considered acceptable. Further checks need to be carried out for structural integrity during fire and concrete spalling, and that ventilation systems can accommodate the smoke from burning pipes. The water volume in the circuitry is a few cubic meters, risk of excess water vapour or local flooding is low.

All exposed pipes need to be considered replaced by non-flammable material or cast in mass concrete. The Crossrail design has the details.

3.2 Sprayed concrete liner

For tunnels that are excavated using drill-and-blast method or road header, absorber pipes can be incorporated with the sprayed concrete linings (SCL), i.e., between the outer sprayed concrete and the in-situ inner concrete lining. The design of SCL tunnel at CLIC is unknown. However, there are multiple projects in Europe have tested the SCL system. See photos below for two examples. Installation of a common geotextile between the two linings is a standard process in tunnels, its installation comes with little additional efforts.

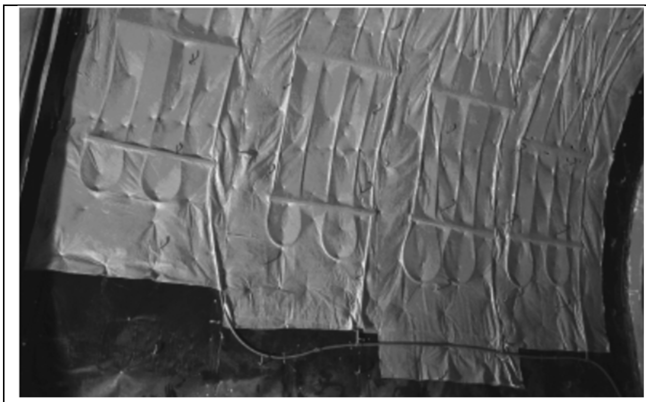	**Lainzer tunnel, Vienna** The pipes were attached to a geofabric with was then pinned inside the primary lining. Then secondary lining is applied. Four absorber loops with collection pipe are shown on the left.
	**Stuttgart- Fasanenhof tunnel, Stuttgart** The pipes are clipped to a set of plastic strips that fastened to the geofabric of the outer tunnel lining with fixing rails and then embedded in the inner tunnel lining.

3.3 Cost considerations

Cost items associated with thermal tunnel installation can be divided into 2 parts, above ground and below ground. It is assumed that the above ground cost will be similar between geothermal boreholes and thermal tunnels, i.e., trenches, pipes, and equipment such as heat pumps and circulation pumps.

For the below ground part, the cost items for thermal tunnel are listed in Table 3. For closed loop boreholes, the cost will be borehole drilling, pipe installation and testing, header to manifold.

Typical installation cost of closed loop boreholes in London are: a 100m borehole costs £5 to £7K; a 200m borehole costs £18K. It does not include equipment cost.

Table 3 Cost items for thermal tunnel installation

	Cost Items	Energy tunnel liner	Data of Dec. 2010 for Crossrail
1	Absorber pipe	PEXa pipes, 20mm OD, SDR11, 5 to 10m per segment	£145/m tunnel, covers joints
2	Prefabrication and Segment casting	modification of segment mould to incorporate pipes (e.g., the supporting system, box-out connections between segments)	£160/m tunnel
3	Segment connection fitting part	Joint coupling for pipes	Covered in item 1
4	Ring to ring connection pipes	Pipe are exposed inside tunnel, need to meet fire safety station. Metal is expected	Unknown
5	Isolation valves for individual ring loop, isolation valves for headers	Valves for control/isolate flow to individual rings	Unknown
6	Labour to perform connections of the segment during tunnelling	1 person-day per 30m	Assuming the TBM advances at 30m a day, labour cost £200 a day.
7	Labour to perform connections between rings and testing	This can be done during fitout	Unknown
8	Labour to perform connections of headers and testing	This can be done during fitout	Unknown
9	Header flow and return	90mm ducts, pipe length for reverse return arrangement requires 1800m long pipes for 600m tunnel	£98m/m tunnel
10	Lay out headers, and cast them in concrete	Connect header with loop circuit, to meet fire safety requirement, the head pipes need to be casted in concrete	Unknown
11	Heat exchanges to isolate tunnel and flow to surface	Heat exchanger functions as hydraulic breaker, and boost temperatures	Unknown
12	*Heat pumps*	*Above ground elements*	*Excluded*
13	Pipe to run from tunnel to ground level	90mm delivery pipes down the shaft	Unknown
14	Pipe to run from ground level to users (excavation and material)	*Above ground elements*	*Excluded*
15	Circulation pumps	*Above ground* and below ground elements	Unknown

Without adding the unknown cost, for a 600m tunnel to be converted to energy geostructure, the estimated cost is £243K. For 35nr boreholes, it costs £210K. However, if the tunnel is running efficiently as the boreholes with balanced loads of heating and cooling, the 600m tunnel could have a capacity equivalent to 70nr or more boreholes, the latter will cost £420K. On this basis, the tunnel is more cost-efficient than the boreholes, but we have under-estimated the tunnel cost. Our comparison is based on our UK experience. We understand that a closed borehole system has been constructed in ZAC 'Ferney-Voltaire'. It is recommended that the cost price and energy performance should be obtained from the site for proper cost comparison.

Saving of ventilation cost for warm tunnel is another possible benefit. It estimated that the for the deep tunnel of Turin–Lyon new railway, if thermal tunnel is used, the cooling ventilation cost saving is €10K to €20K per kilometre per year. It is noted that the tunnel temperature is significantly higher than CLIC (Barla & Di Donna, 2018).

Payback time depends on system operation (energy delivered over a year) and cost of other energy methods. (Moormann, et al., 2016) claims that 9 to 15 years payback time is possible, however the assumptions used in the analyses are unknown.

4. Discussions

4.1 Thermal tunnel use and heating sources

To run the thermal tunnel in a cold tunnel environment, thermal load balance is essential to ensure the sustainability of the system. For climate in Switzerland, cooling load for residential building almost non-exist. Cooling demand of commercial and office buildings is likely.

4.2 Projects with thermal tunnel constructed

New tunnels are built around the world as part of urban and infrastructure development every year. Additional investment to integrate the geothermal system in the tunnel is relatively small compared to the project cost. The revenue comes from selling the energy harvested by the system. However, CERN may also consider carbon saving, ventilation cost reduction (Biotto, et al., 2013), and future proofing. The lifetime of tunnels is 100 years or more, this long operational need could help to smooth out the pain of long payback time.

Table 4 lists the existing thermal tunnel projects. The high heat extraction rates at Turin metro tunnels are due to ground flow.

Performance or test data is scarce. Stuttgart-Fasanenhof and Jenbach are two thermal tunnels which have been measurement data of soil and tunnel temperatures for four years. Figure 12 shows the heating operational data at Stuttgart-Fasanenhof tunnel between 09/03 and 15/03/2012. The heat extraction rate is 20 W/m^2 for 8 hours a day. This was achieved by setting the inlet temperature to 0.5°C. Tunnel air and soil temperatures are somehow affected by the operation.

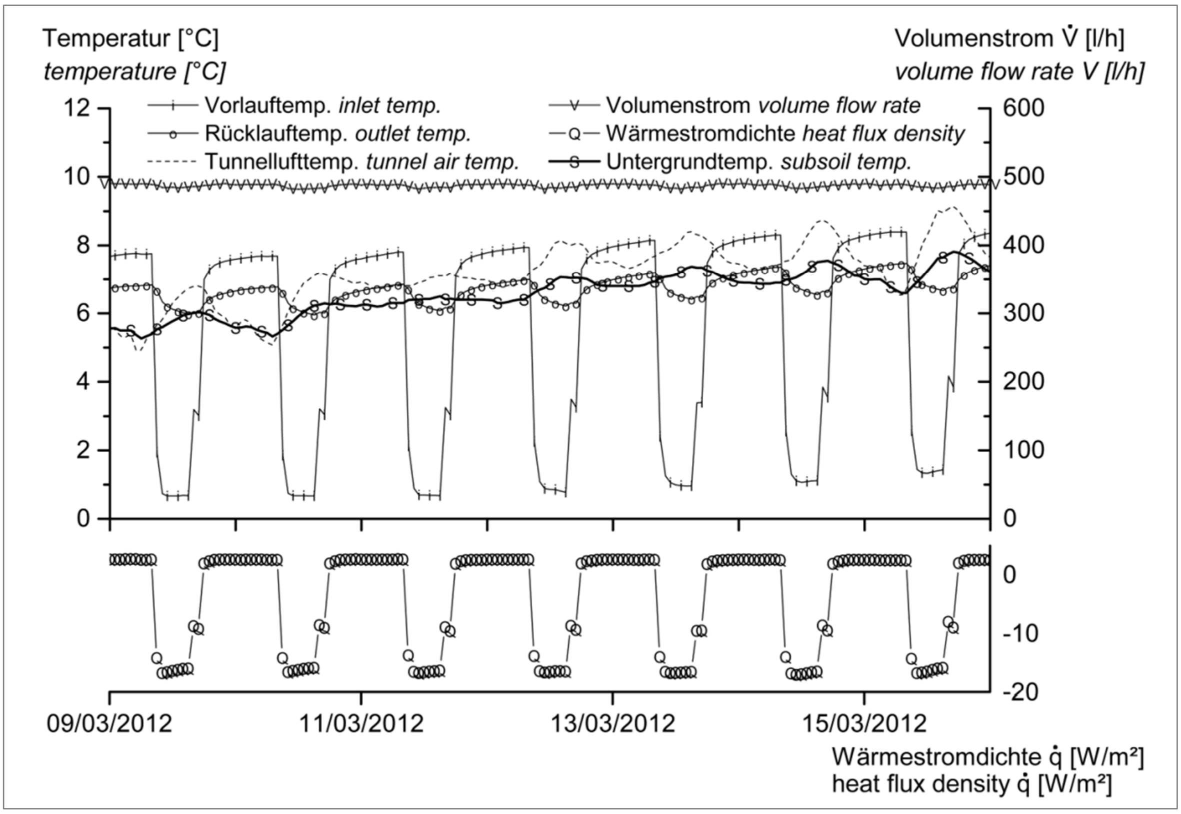

Figure 12 Stuttgart-Fasanenhof tunnel during winter (Moormann, et al., 2016)

At the Jenbach tunnel, 20 to 25 kW heat rejection rate (cooling operation) was operated during the summer months, which equates to about 10 to 12 W/m² given the thermal system area is 2000m^2. As shown in Figure 13, during early August and mid October 2013, the inlet temperature of the loop is 2 to 5°C, and the outlet temperature is 5 to 10°C higher.

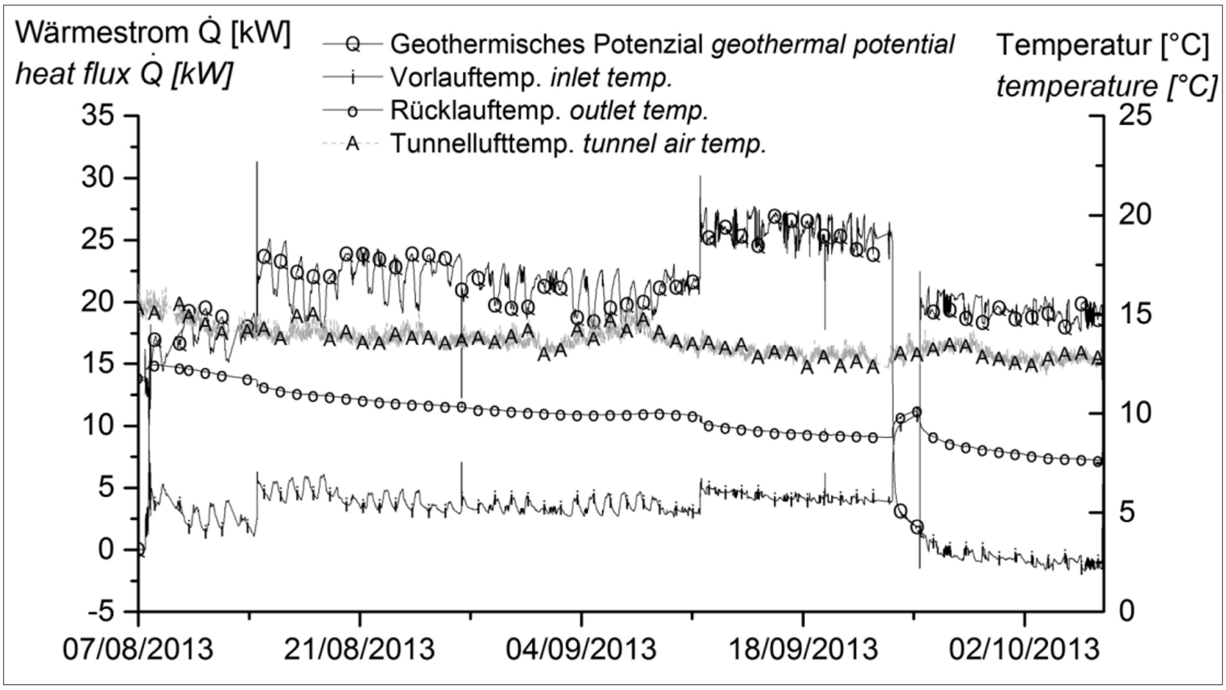

Figure 13 Test of cooling operation at the Jenbach tunnel in 2013 (Moormann, et al., 2016)

4.3 Lessons learnt

A few lessons learn from past projects:

- Starting the thermal tunnel design early with tunnel design team to allow for space proofing and other design changes
- Adding thermal tunnel element in the original tender. This is to avoid higher asking price when the work is added to the scope after contractor has been appointed
- Using a trial section to demonstrate and smooth out the design and installation procedure.

Table 4 Thermal tunnel projects in Europe and Asia

Name	Location	Country	Tunnel use	Tunnel type	Tunnel lining	Depth to tunnel (m)	Thermal activated tunnel length (m)	Activated area (m^2)	Power output (W/m^2)	Applications
Seocheon tunnel	Seocheon County	South Korea	Abandoned	Cold	SCL			90		a test bed of six pilot energy textile modules with various configurations was constructed in an abandoned railroad tunnel
Linchang	Inner Mongolia	China	Rail	Cold	SCL					experiments on factors, such as flow rate, inlet temperature and pipe arrangement, affect the heat transfer
Stuttgart-Fasanenhof (2011)	Stuttgart	Germany	Rail	Cold	SCL	10	20 (2 tunnel sections, 10m each)	360	3 to 8	Cooling tests, tunnel height 9.2m, width 7.2m. With fixed inlet temperatures for the absorbers showed variations between 5W/m² and 37 W/m² in cooling effect per absorber heat exchange area. The highest power output was obtained at the beginning of the phase. The thermal output decreased with time, partly due to the temperature increase of the absorber surroundings. An influence of the tunnel air temperature could be seen. (Moormann, et al., 2016); (Bidarmaghz & Narsilio, 2018)
Rosenstein tunnel B10 (2015)	Stuttgart	Germany	Road	Cold	SCL	na	14 blocks	3300	56	Heating test for 56kW (Csesznák, et al., 2016)
Jenbach Tunnel (2008)	Tyrol	Austria	Rail	Warm	Precast	16	54 (27 rings)	2030	18 to 40	pipe circuits were connected along the invert to the escape shaft (Franzius & Pralle, 2011)
Lainzer tunnel (2003)	Vienna	Austria	Metro	Cold-Warm	SCL					LT22, 'energy geotextile'. Air conditioning of operating rooms (Adam & Markiewicz, 2009)

Name	Location	Country	Tunnel use	Tunnel type	Tunnel lining	Depth to tunnel (m)	Thermal activated tunnel length (m)	Activated area (m^2)	Power output (W/m^2)	Applications
Turin Metro, Line 1 South Extension	Turin	Italy	Metro	cold-warm	Precast	12	2 rings	120	48 to 51	GW flow enhances power output. Predicted capacity 53 W/m^2 winter heat extraction and 74W/m^2 summer heat rejection (Barla & Di Donna, 2018)
Turin Metro, Line 2	Turin	Italy	Metro	cold-warm	Precast	20 to 38	Feasibility	Feasibility	1 MW of thermal energy per km tunnel	feasibility study, groundwater flow and use of Enertun segments enhances heat exchange. (Barla, et al., 2019)
Warsaw Metro, Line 2	Warsaw	Poland	Metro		Precast		Feasibility	Feasibility		feasibility study shows that the thermal activation of two 1.6 km long tunnels could exchange up to 5.3 GWh and 5.8 GWh in the heating and cooling season, respectively.
Crossrail	London	England	Metro	Warm	Precast	20 to 30	Feasibility	Feasibility	10 to 30	feasibility study
Katzenberg tunnel (2007)	Karlsruhe	Germany	Rail	Cold			5 segments	60	10 to 20	Tested for 5 months

4.4 Other geothermal options

- The base slabs of the tunnel can be thermally activated, power output is 5W/m^2 (Loveridge, et al., 2017).
- Arup has developed a deep single geothermal well for district heating, however itself is a big undertaking and has little to do with tunnel.

5. Conclusions and Recommendations

Tunnels have a large soil-structure surface and involve a large volume of ground mass, the surrounding soil of tunnel structures can be used for energy storage and an energy source. Pilot projects of converting Metro, road, and rail tunnels to an energy geo-structure have been implemented in Europe and Asia.

CLCI tunnel is a scientific experiment tunnel. It is significantly deeper than the urban transport tunnels. Our study concluded that the tunnel can be thermally activated using the existing thermal tunnel design with some modification. Heat exchangers or similar are needed to form a hydraulic break between surface and tunnel circuits. Without in-tunnel heat sources and ignoring nature heat flux from tunnel air to the ground, the tunnel is a 'cold tunnel'. In order to for a closed system to be sustainable, there is a need to energy balance, i.e. the heat extracted by the system needs to be balanced by heat rejection, the system can be either run intermittently at low heat recovery rate and allow it to recovery with heat flux from geothermal and tunnel air, or actively reject heat to the system during summer.

The lower bound of energy output of the thermal tunnel is 10W/m^2, this is likely to be an underestimate as tunnel air or heat ejection is not considered. A 600m thermally activated tunnel is similar to that of 35nr 100m borehole in term of ground heat exchange rate. For like-to-like comparison, i.e. the tunnel is to run with a balanced load, the tunnel can produce 20-30W/m^2, which is similar to 70nr or more GSHP boreholes.

The following work is recommended to further the design:

- To carry out structural analysis using 3D thermal-mechanical coupled model: at CLIC the tunnel liner is in a larger stress field compared with shallow metro tunnel, thermal effect on the concrete liner needs to be closely assessed. Coupled thermal-mechanical (soil structure) analysis is recommended.
- To firm up the method to achieve thermal balance for the system. It is important to use the thermal tunnel to supply both building heating and cooling .
- The thermal tunnel design is technically feasible. However, CAPEX, OPEX and lifetime cost-benefit analyses are required to provide the basis for an informed decision.

References

Adam, D. & Markiewicz, R., 2009. Energy from earth-coupled structures, foundations, tunnels and sewers. *Geotechnique,* 59(3), pp. 229-236.

Barla, M. et al., 2019. Feasibility study for the thermal activation of Turin Metro Line 2. In: V. &. C. Peila, ed. *Tunnels and Underground Cities: Engineering and Innovation meet Archaeology, Architecture and Art.* London: Taylor & Francis Group, pp. 231-240.

Barla, M. & Di Donna, A., 2018. Energy tunnels: concept and design aspects. *Underground Space (China),* pp. 268-276.

Bidarmaghz, A. & Narsilio, G., 2018. Heatexchangemechanismsinenergytunnelsystems. *GeomechanicsforEnergyandtheEnvironmen,* Volume 16, p. 83–95.

Biotto, C., Eckford, D. & Chen, Q., 2013. *Efficient tunnel cooling using tunnel wall heat extraction.* s.l., s.n.

Bowden, G., 2003. *Linear Collider Collaboration Tech Notes: Tunnel Wall Heat Transfer,* Stanford: Stanford University.

Brandl, H., 2006. Energy foundations and other thermo-active ground structures. *Géotechnique,* 56(2), p. 81–122.

CERN, 2018. *CLIC Project Implementation Plan, CERN Yellow Reports: Monographs, ISBN 978–92–9083–515–8.* Geneva: CERN.

Claudet, S., 2022. *CERN energy management, energy efficiency analysis & selected project,* Geneva: presentation at CERN-Arup meeting in Feb 2022.

Csesznák, A., Järschke, R. & Wittke, M., 2016. B 10 Rosenstein Tunnel – Designing a geothermal energy system in a spa protection area. *Geomechanik und Tunnelbau,* 9(5), pp. 458-466.

Franzius, J. N. & Pralle, N., 2011. Turning segmental tunnels into sources of renewable energy. *Proceedings of the Institution of Civil Engineers – Civil Engineering,* p. 35–40.

Guglielmetti, L. & Moscariello, A., 2021. On the use of gravity data in delineating geologic features of interest for geothermal exploration in the Geneva Basin (Switzerland): prospects and limitations. *Swiss Journal of Geosciences,* p. 114:15.

Institute of Civil Engineering, 2016. *ICE Specification for piling and embedded retaining walls.* 3 ed. London: Thomas Telford.

Loveridge, F., Low, J. & Powrie, W., 2017. Site investigation for energy geostructures. *Quarterly Journal of Engineering Geology and Hydrogeology,* 50(2), p. 158–168 .

Moormann, C. et al., 2016. *Tunnel geothermics – International experience with renewable energy concepts in tunnelling.* s.l., Wilhelm Ernst and Sohn, pp. 467-480.

Nicholson, D. P. et al., 2014. The design of thermal tunnel energy segments for Crossrail, UK. *Proceedings of the Institution of Civil Engineers-Engineering Sustainability,* 167(3), p. 118–134.

Nicholson, D. P. et al., 2014. The design of thermal tunnel energy segments for Crossrail, UK. *Proceedings of the Institution of Civil Engineers: Engineering Sustainability,* 167(3).

Nicholson, D. P., Chen, Q., Pillai, A. & Chendorain, M., 2013. *Developments in thermal piles and thermal tunnel lining for city scale GSHP systems.* Stanford University, Thirty-Eight Workshop on Geothermal Reservoir Engineering.

Rybach, L., 1992. Geothermal potential of the Swiss Molasse Basin. *Eclogae Geologicae Helvetiae,* Volume 85, p. 733–744.

Stemmle, R., Menberg, K., Rybach, L. & Blum, P., 2022. Tunnel geothermics – A review. *Geomechanik und Tunnelbau,* pp. 104 -111.

Attachments